

Expanded View Figures/Table

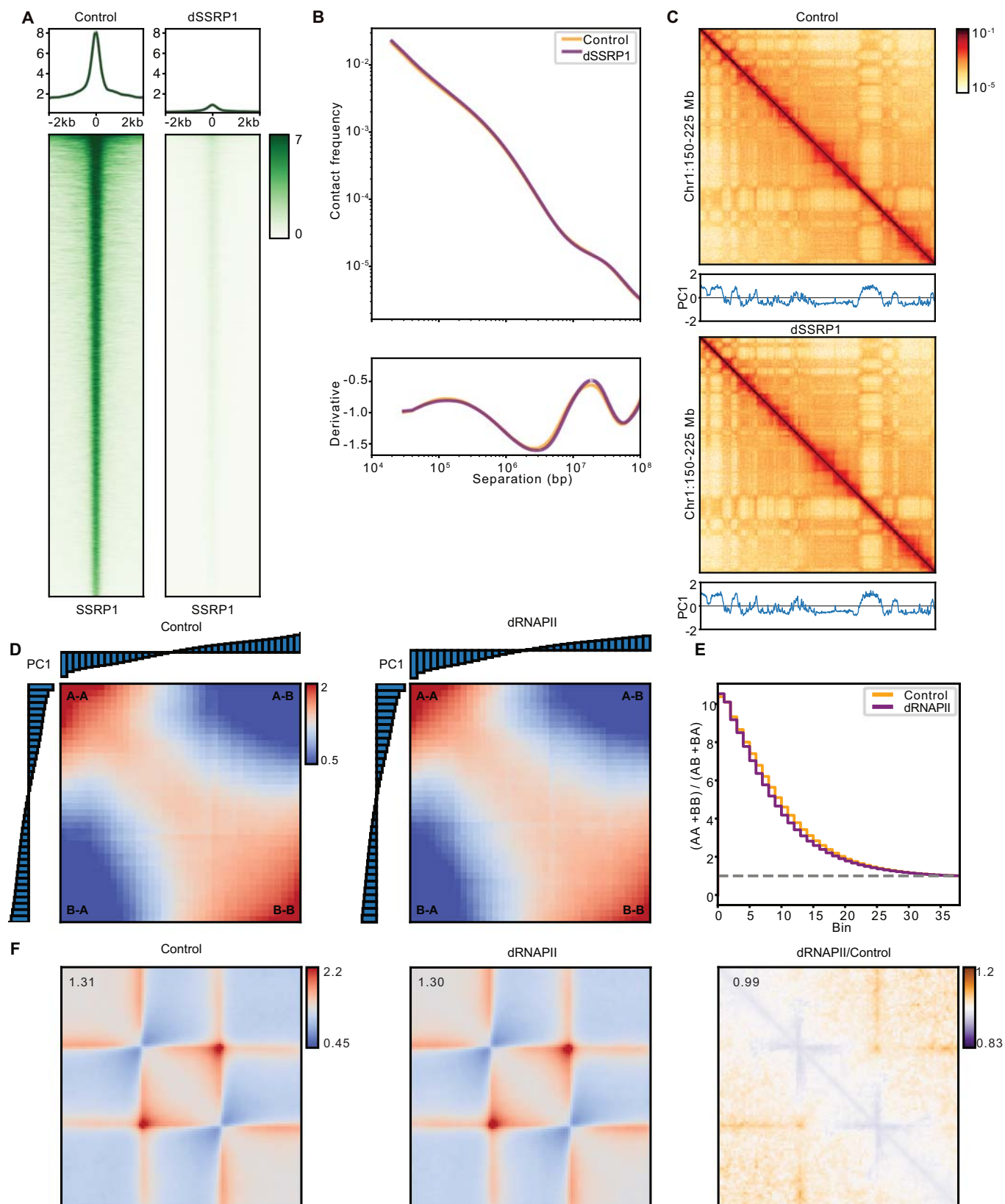
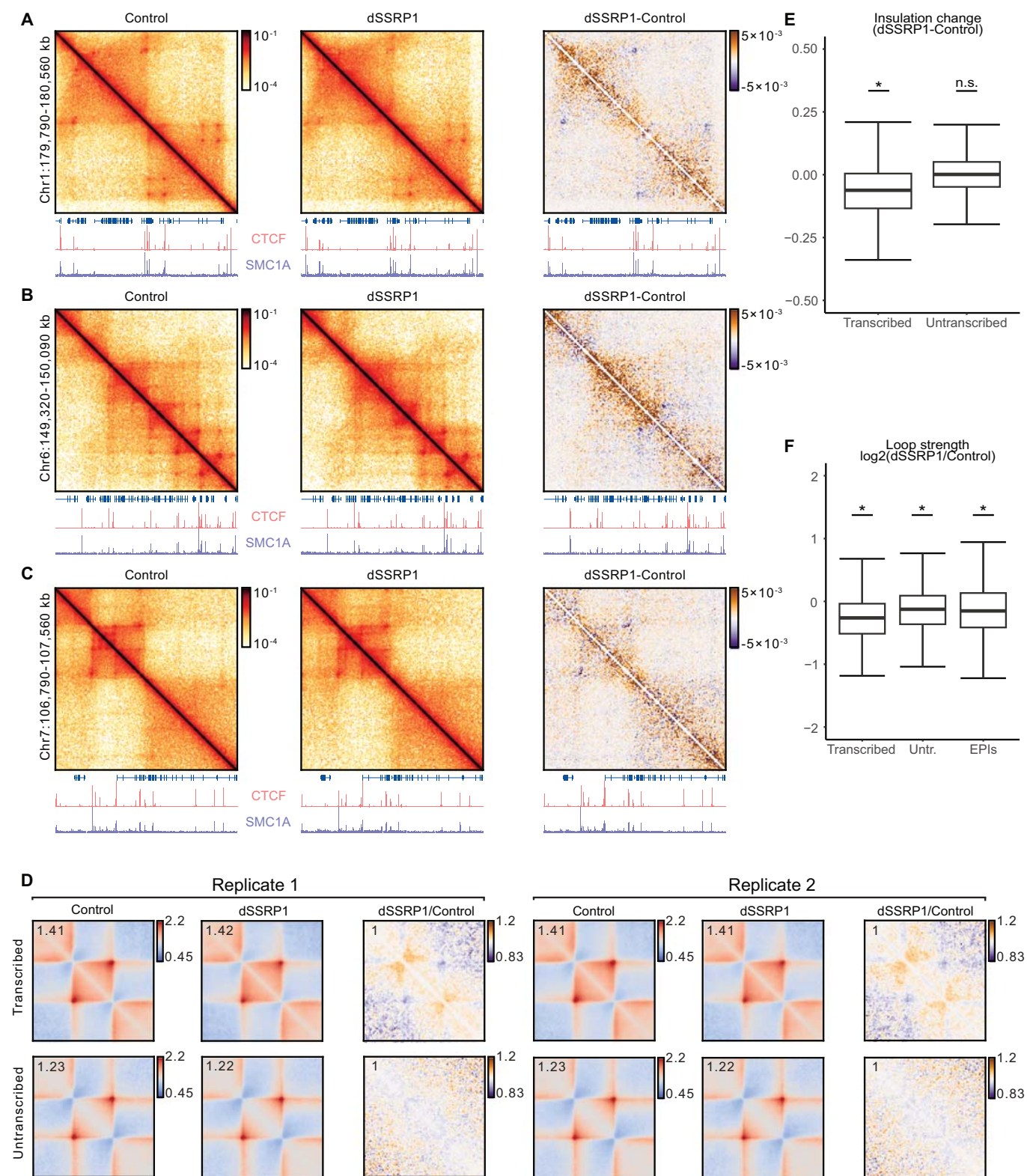




Figure EV1. Rapid depletion of FACT leads to changes in 3D genome organization that are not secondary to changes in transcription.

(A) SSRP1 ChIPmentation signal in control (left) and SSRP1-depleted (right) K562 cells. ChIPmentation data show the average of 2 biological replicates. (B) Micro-C contact frequency decay as a function of genomic distance (top) and its first derivative (bottom) in control (orange) and SSRP1-depleted (purple) cells. Data as in Fig. 1A. (C) Micro-C contact matrices (100 kb resolution) of an exemplary region on chromosome 1 in control (left) and SSRP1-depleted (right) cells. Below is the Eigenvector indicating A compartment (> 0) or B compartment (< 0). Data as in Fig. 1A. (D) Saddleplots displaying observed/expected intra- and intercompartment interactions of genomic regions stratified into 39 bins by Eigenvector decomposition in control (left) and RNAPII-depleted cells (right). Histograms show Eigenvalues of stratified bins. Micro-C data show the average of 2 biological replicates. (E) Step-plot showing the saddle strength profile (intracompartamental/intercompartmental interactions) in control (orange) and RNAPII-depleted (purple) cells. Data as in (D). (F) Mean observed/expected contact frequencies at TADs ($n = 2831$) in control (left) and RNAPII-depleted (middle) cells and their relative differences (right; purple indicates enriched contacts in control cells; orange indicates enriched contacts in RNAPII-depleted cells). TADs are rescaled to the same size. Average signal is reported in the top left. Data as in (D).



◀ **Figure EV2. Rapid depletion of FACT leads to significant changes in 3D genome organization that are consistent across genomic regions and replicates.**

(A) Micro-C contact matrices (5 kb resolution) of an exemplary region on chromosome 1 in control (left) and SSRP1-depleted (middle) K562 cells and their absolute differences (right; purple indicates enriched contacts in control cells; orange indicates enriched contacts in SSRP1-depleted cells). Gene annotation and ChIPmentation tracks for CTCF and SMC1A in control (left and right) and SSRP1-depleted cells (middle) are shown at the bottom. Data as in Fig. 2A. (B) Same as (A) for an exemplary region on chromosome 6. (C) Same as (A) for an exemplary region on chromosome 7. (D) Mean observed/expected contact frequencies at transcribed (top) and untranscribed (bottom) TADs in independent replicates of control (left) and SSRP1-depleted (middle) cells and their relative differences (right; purple indicates enriched contacts in control cells; orange indicates enriched contacts in SSRP1-depleted cells). TADs are rescaled to the same size. Average signal is reported in the top left. Data as in Fig. 2A. (E) Relative differences in insulation scores at transcribed (left; two-sided Wilcoxon rank-sum test; $n = 1811$, $P < 2.2e-16$) and untranscribed (right; two-sided Wilcoxon rank-sum test; $n = 1948$, $P < 2.2e-16$) TAD boundaries between control and dSSRP1-depleted cells. Boxplots show the interquartile range (IQR) and median of the data; whiskers indicate the minima and maxima within $1.5 \times \text{IQR}$; asterisks indicate statistical significance ($P < 0.05$); n.s. = non-significant. Data as in Fig. 2A. (F) Same as (E) for CTCF loop strength at transcribed (left; two-sided Wilcoxon rank-sum test; $n = 657$, $P < 2.2e-16$) and untranscribed (Untr.; middle; two-sided Wilcoxon rank-sum test; $n = 900$, $P < 2.2e-16$) TAD boundaries and enhancer-promoter interactions (right; two-sided Wilcoxon rank-sum test; $n = 423$, $P < 9.718e-11$).

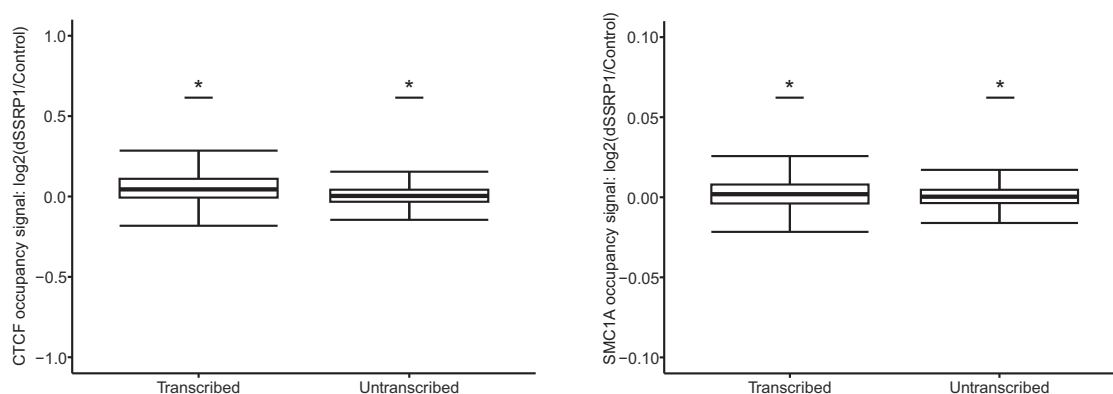


Figure EV3. The effects of FACT depletion on TAD organization are not dependent on reduced CTCF and cohesin occupancy.

Relative differences in CTCF (left panel) and SMC1A (right panel) occupancy between control and dSSRP1-depleted K562 cells in transcribed (left box; two-sided Wilcoxon rank-sum test; $n = 22,681$, $P < 2.2 \times 10^{-16}$) and untranscribed (right box; two-sided Wilcoxon rank-sum test; $n = 20,099$, $P < 2.2 \times 10^{-16}$) regions. Boxplots show the interquartile range (IQR) and median of the data; whiskers indicate the minima and maxima within $1.5 \times \text{IQR}$; asterisks indicate statistical significance ($P < 0.05$). Data as in Fig. 3.

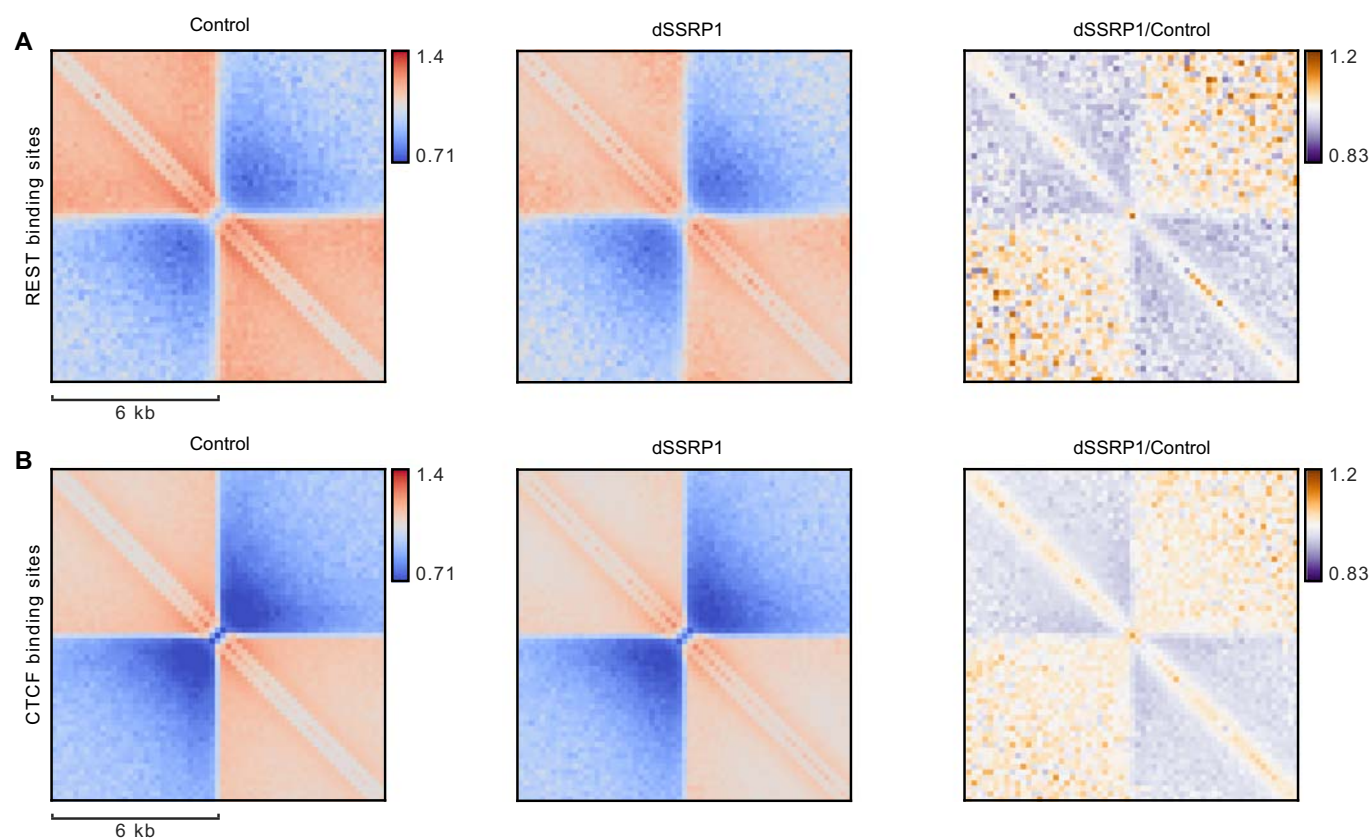


Figure EV4. Local insulation at REST and CTCF binding sites.

(A) Mean observed/expected contact frequencies at REST binding sites (that do not overlap with CTCF binding sites; $n = 13,387$) in control (left) and SSRP1-depleted (middle) K562 cells and their relative differences (right; purple indicates enriched contacts in control cells; orange indicates enriched contacts in SSRP1-depleted cells). Note that insulation shown here extends over much shorter distances compared to insulation at CTCF-bound TAD borders shown in Fig. 1C. Data as in Fig. 2A. (B) Same as (A) at all CTCF binding sites across the genome (including CTCF binding sites that do not overlap with TAD borders; $n = 57,154$).

Table EV1. Micro-C mapping, deduplication, and contact statistics from 2 merged biological replicates.

	Control		dSSRP1	
	Read number	Percentage	Read number	Percentage
Total read pairs	2,033,336,706	100	1,830,972,576	100
Mapped read pairs	1,821,115,104	89.6	1,626,027,133	88.8
Duplicate read pairs	304,308,463	26.6	260,134,033	25.8
Valid <i>trans</i> read pairs	152,853,931	13.4	127,161,826	12.6
Valid <i>cis</i> read pairs	686,790,761	60	620,232,513	61.6

Percentages in top two rows are relative to total number of read pairs; percentages in bottom three rows are relative to total number of uniquely aligned read pairs.